

# Principal Component Regression for Forensic Age Determination Using the Raman Spectra of Teeth

---

Osmani, Aziz; Par, Matej; Škrabić, Marko; Vodanović, Marin; Gamulin, Ozren

Source / Izvornik: **Applied Spectroscopy**, 2020, 74, 1473 - 1485

Journal article, Published version

Rad u časopisu, Objavljena verzija rada (izdavačev PDF)

<https://doi.org/10.1177/0003702820905903>

Permanent link / Trajna poveznica: <https://urn.nsk.hr/urn:nbn:hr:127:211195>

Rights / Prava: [Attribution-NonCommercial-NoDerivatives 4.0 International/Imenovanje-Nekomercijalno-Bez prerada 4.0 međunarodna](#)

Download date / Datum preuzimanja: **2024-05-21**



Repository / Repozitorij:

[University of Zagreb School of Dental Medicine Repository](#)



# Principal Component Regression for Forensic Age Determination Using the Raman Spectra of Teeth

Aziz Osmani<sup>1,\*</sup>, Matej Par<sup>2,3,\*</sup> , Marko Škrabić<sup>4,5</sup> ,  
Marin Vodanović<sup>6</sup>, and Ozren Gamulin<sup>4,5</sup>

Applied Spectroscopy  
2020, Vol. 74(12) 1473–1485  
© The Author(s) 2020  
Article reuse guidelines:  
sagepub.com/journals-permissions  
DOI: 10.1177/0003702820905903  
journals.sagepub.com/home/asp



## Abstract

Raman spectra of mineralized tooth tissues were used to build a principal component regression (PCR) age determination model for forensic application. A sample of 71 teeth was obtained from donors aging from 11 to 76 years. No particular selection criteria were applied; teeth affected with various pathological processes were deliberately included to simulate a realistic forensic scenario. In order to comply with the nondestructive specimen handling, Raman spectra were collected from tooth surfaces without any previous preparation. Different tooth tissues were evaluated by collecting the spectra from three distinct sites: tooth crown, tooth neck, and root apex. Whole recorded spectra ( $3500\text{--}200\text{ cm}^{-1}$ ) were used for principal component analysis and building of the age determination model using PCR. The predictive capabilities of the obtained age determination models varied according to the spectra collection site. Optimal age determination was attained by using Raman spectra collected from cementum at root apex ( $R^2$  values of 0.84 and 0.71 for male and female donors, respectively). For optimal performance of that model, male and female donors had to be analyzed separately, as merging both genders into a single model considerably diminished its predictive capability ( $R^2 = 0.29$ ).

## Keywords

Raman spectrometry, principal component analysis, PCA, principal component regression, PCR, age determination, forensic dentistry

Date received: 10 October 2019; accepted: 10 January 2020

## Introduction

Age determination is one of the most common forensic procedures which has a wide range of applications, including identifications of accident victims, crime investigations, and social benefit regulations. Among various types of tissues available for forensic analyses, mineralized dental tissues are advantageous due to their high resistance to postmortem decomposition.<sup>1</sup> In forensic dentistry, three distinct approaches can be used for age determination: (i) the assessment of tooth morphological features by visual inspection or radiography, (ii) the evaluation of tooth histological characteristics using microscopy, and (iii) the evaluation of biochemical composition of tooth tissues using various analytical methods, including Raman spectrometry.<sup>2</sup> Whereas morphological and histological methods are routinely practiced in the contemporary forensic dentistry,<sup>1</sup> the biochemical analyses are still more pertinent to the experimental domain.<sup>3</sup> However, the biochemical means of age estimation offer important advantages over the conventional approaches, rendering them useful

complementary methods.<sup>4</sup> For example, biochemical analyses require very small amounts of mineralized tissues and are applicable in cases of extensively damaged teeth.<sup>5</sup>

<sup>1</sup>Community Health Center “Kutina”, Kutina, Croatia

<sup>2</sup>Department of Conservative and Preventive Dentistry, Center for Dental Medicine, University of Zurich, Zurich, Switzerland

<sup>3</sup>Department of Endodontics and Restorative Dentistry, School of Dental Medicine, University of Zagreb, Zagreb, Croatia

<sup>4</sup>Department of Physics and Biophysics, School of Medicine, University of Zagreb, Zagreb, Croatia

<sup>5</sup>Center of Excellence for Advanced Materials and Sensing Devices, Research Unit New Functional Materials, Zagreb, Croatia

<sup>6</sup>Department of Dental Anthropology, School of Dental Medicine, University of Zagreb, Zagreb, Croatia

\*These authors contributed equally to this work.

## Corresponding author:

Matej Par, University of Zurich, Center for Dental Medicine, Plattenstrasse 11, Zurich 8032, Switzerland.  
Email: mpar@sfzg.hr

Raman spectrometric analyses of dental hard tissues have been performed in various studies, including evaluations of enamel mineralization,<sup>6–8</sup> early caries detection,<sup>9–11</sup> compositional differences between primary and permanent teeth,<sup>12</sup> and mapping of the spatial distribution of organic and inorganic components in dental tissues.<sup>13</sup> However, only two studies have employed Raman spectrometry to relate the aging-dependent compositional changes in tooth tissues with the donor's age for forensic purposes.<sup>14,15</sup> In these studies, Raman spectra were collected from surfaces of longitudinally sectioned sound teeth and partial least squares regression was performed to correlate predefined compositional variables obtained from Raman spectra with tooth donor's age. The aforementioned studies were based on ideal case scenarios in which Raman spectra were collected from standardized, flat-cut specimen surfaces obtained from healthy teeth. In order to complement these proof-of-principle studies, the present investigation simulated a more realistic scenario by including the teeth that were affected by common pathological processes, such as periodontal disease and dental caries. In addition, the spectral analysis in the present study was performed considering the whole Raman spectra, in contrast to the aforementioned studies which analyzed various combinations of parameters characterizing individual vibrational bands.<sup>14,15</sup> Instead of cutting the teeth to analyze their internal structure, Raman spectrometry in the present study was performed on more accessible external surfaces of teeth. The described approach was adopted in order to evaluate the feasibility of Raman spectrometric age determination by using nondestructive handling of teeth that were affected by various pathologies. The research hypotheses were: (i) Raman spectra obtained from teeth would correlate with donor's age and (ii) different sites of spectra collection (tooth crown, tooth neck, and root apex) would influence the accuracy of age estimation models.

## Materials and Methods

The teeth were extracted at the university clinic of the School of dental medicine, Zagreb, Croatia. As an integral part of the regular practice of informed consent at the clinic, all donors agreed that their teeth can be retained and used for research. No personal data and other identifying information about donors have been disclosed to the investigators. The collection and handling of biological material were conducted in full accordance with the World Medical Association Declaration of Helsinki regarding ethical principles for medical research involving human subjects. The soft tissues that remained after tooth extraction were removed using a plastic brush and the teeth were disinfected by soaking in a 1% formaldehyde solution for 24 h. Thereafter, the teeth were stored dry in dark containers at room temperature ( $23 \pm 3^\circ\text{C}$ ) in the archive of

the Department of Dental Anthropology of the School of Dental Medicine, University of Zagreb, Croatia.

The sample of 71 teeth used for this study was obtained by a random draw from the aforementioned archive. The age of tooth donors ranged between 11 and 76 years (Table I). The teeth had been extracted due to various indications, most common being periodontitis (51%) and failed endodontic treatment (39%). To simulate a forensic analysis of teeth at different postextraction time periods, the time span between extraction and performing Raman spectrometric measurements ranged between 0.1 and 5.5 years. No special selection criteria were applied; teeth affected with various pathological processes were deliberately included to simulate a realistic sample. The visual appearance of teeth affected by the most common pathologies is represented in Fig. 1.

Raman spectra were recorded using an FT-Raman accessory of the Spectrum GX spectrometer (Perkin Elmer, USA) equipped with a neodymium-doped yttrium aluminum garnet (Nd : YAG) laser of 1064 nm wavelength. Each spectrum was recorded by averaging 100 scans in the spectral range between 3500 and  $200\text{ cm}^{-1}$  and with a spectral resolution of  $4\text{ cm}^{-1}$ . Spectra were collected from three distinct sites on each tooth: crown, neck, and apex (Fig. 2). At each site, an area of 2.5 mm in diameter was chosen, over which the excitation laser spot (0.25 mm in diameter) was moved in a scanning motion to collect Raman spectra from 10 different positions. This was done in order to account for local heterogeneities of mineralized tooth tissues. Therefore, a total of 30 spectra per tooth were collected (three sites, 10 spectra). The spectra were stored in a data set and connected with the donor's age and collection site.

All spectra were baseline corrected and normalized using the peak at  $960\text{ cm}^{-1}$  (symmetric  $\text{PO}_4$  stretching) to exclude possible differences caused by variations in recording conditions. Whole Raman spectra ( $3500\text{--}200\text{ cm}^{-1}$ ) were used for principal component analysis (PCA) and principal component regression (PCR) with three to seven principal components. To evaluate the capability of PCA for separating the spectra according to tooth donor's age, the spectra were divided into seven age groups (Table II). This grouping was used to color-code the data in PCR scores plots in order to visually distinguish the separation of spectra according to the donor's age. PCR was used to establish a relationship between the recorded spectra and the donor's age. PCA and PCR were performed using a model built within MATLAB 2010 (The MathWorks Inc., USA) and its add-on PLS\_Toolbox (Eigenvector Research, USA). An advanced preprocessing technique, generalized least squares weighting, was employed before the PCA modeling to remove information from the interfering compounds without losing relevant aging-related variability among the data.<sup>16–19</sup> Separate PCA/PCR models were built according to the spectra collection site and donor's

**Table 1.** Characteristics of teeth used in this study.

Specimen no.	Gender	Tooth type according to ISO 3950 notation	Donor age (years)	Time between extraction and spectra collection (years)	Reason for extraction
1	M	14	15	0.2	Ortho
2	M	14	16	3.5	Ortho
3	M	35	16	3.5	Endo
4	M	47	22	0.2	Endo
5	M	18	23	0.1	Imp/ret
6	M	37	31	0.1	Endo
7	M	37	32	0.2	Endo
8	M	47	35	0.3	Endo
9	M	27	44	0.1	Endo
10	M	45	45	2.9	Endo
11	M	33	46	2.5	Perio
12	M	14	47	4.2	Endo
13	M	21	49	0.3	Perio
14	M	48	49	0.3	Perio
15	M	25	52	3.9	Perio
16	M	46	52	0.2	Endo
17	M	47	54	0.3	Perio
18	M	15	55	3.7	Perio
19	M	27	55	4.0	Perio
20	M	21	58	4.2	Perio
21	M	37	58	4.2	Perio
22	M	17	58	4.2	Endo
23	M	13	59	3.8	Perio
24	M	17	64	0.4	Perio
25	M	44	64	0.1	Perio
26	M	36	65	0.3	Endo
27	M	17	67	0.2	Endo
28	M	27	67	0.1	Perio
29	M	45	68	4.0	Perio
30	M	13	70	3.8	Perio
31	M	12	73	3.7	Perio
32	M	36	76	0.3	Endo
33	F	24	11	4.0	Ortho
34	F	36	17	0.5	Endo
35	F	35	23	0.3	Ortho
36	F	36	23	0.4	Endo
37	F	47	23	0.5	Endo
38	F	18	26	5.5	Endo
39	F	28	29	0.4	Imp/ret
40	F	28	31	0.3	Endo
41	F	24	35	4.4	Endo
42	F	28	35	0.4	Endo
43	F	11	38	4.5	Perio
44	F	13	38	4.0	Endo

(continued)

Table I. Continued

Specimen no.	Gender	Tooth type according to ISO 3950 notation	Donor age (years)	Time between extraction and spectra collection (years)	Reason for extraction
45	F	27	38	0.6	Perio
46	F	43	39	4.0	Perio
47	F	12	39	4.0	Perio
48	F	18	39	0.6	Endo
49	F	45	39	3.8	Perio
50	F	48	39	0.3	Imp/ret
51	F	22	46	4.1	Perio
52	F	33	46	4.0	Perio
53	F	37	46	0.6	Endo
54	F	36	48	0.1	Endo
55	F	35	49	3.4	Perio
56	F	44	49	3.7	Perio
57	F	27	51	0.5	Perio
58	F	25	53	3.9	Perio
59	F	37	55	0.5	Endo
60	F	27	56	0.5	Perio
61	F	11	58	4.1	Perio
62	F	13	58	3.2	Perio
63	F	34	58	0.2	Perio
64	F	37	58	0.6	Perio
65	F	45	62	4.0	Perio
66	F	17	64	0.5	Endo
67	F	21	64	4.0	Perio
68	F	45	65	4.1	Perio
69	F	26	66	0.6	Perio
70	F	23	69	0.1	Endo
71	F	37	73	0.6	Endo

Ortho: orthodontic extraction; Endo: failed endodontic treatment or inability to perform endodontic treatment; Perio: extraction due to advanced periodontitis; Imp/ret: impacted or retained tooth.

gender, resulting in the following six combinations: apex male, apex female, crown male, crown female, neck male, and neck female. Additionally, spectra from both genders were mixed together in three “joint” models that accounted only for the spectra collection site. All models were cross-validated using the Venetian blind method.

## Results

Representative Raman spectra collected from different tooth sites are shown in Fig. 3. The inorganic part is represented by vibrational bands in the wavenumber range of  $1100\text{--}400\text{ cm}^{-1}$  ( $\text{PO}_4$  and  $\text{CO}_3$  vibrations), while the organic part is represented in the range of  $3100\text{--}1100\text{ cm}^{-1}$  (amide bands and C–H vibrations).<sup>13,20</sup> While the spectra from all three sites featured the same

bands, the inorganic/organic ratio was considerably higher in spectra collected from the crown compared to the other two sites. This reflects the fact that all types of tooth tissue comprise the same basic building blocks, although in various relative amounts. Individual assignments of spectral bands are shown in Table III. From a biochemical perspective, the major component of the inorganic part is carbonated calcium-deficient hydroxyapatite, while most of the organic part consists of collagen.<sup>21,22</sup>

To illustrate aging-related spectral changes, baseline-corrected and normalized spectra collected from the apex of male donors are presented as average spectra for each of the seven age groups (Fig. 4). The changes in the intensity of bands representing both the inorganic and organic components of tooth tissues indicate that it is possible to build a PCA model for distinguishing donor's age using Raman spectra. Also, the spectral changes occurring as a

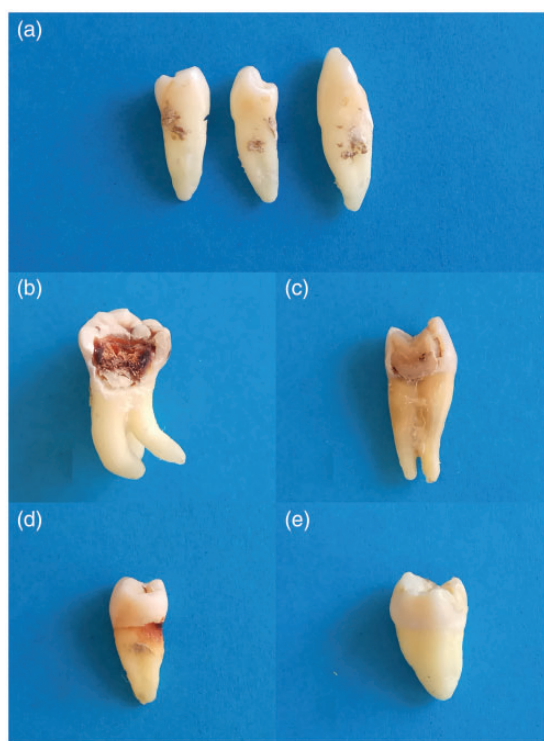


**Figure 1.** Representative specimens of teeth affected to different extents by various pathological processes: (a) sub-gingival calculus reaching up to the mid-root level which is indicative of advanced periodontitis, (b) severe destruction of the tooth crown accompanied by irreversible pulpal inflammation, (c) extensively restored tooth with the discolored root indicating failed endodontic treatment, (d) caries at the level of the tooth neck, and (e) sound third molar extracted due to impaction.

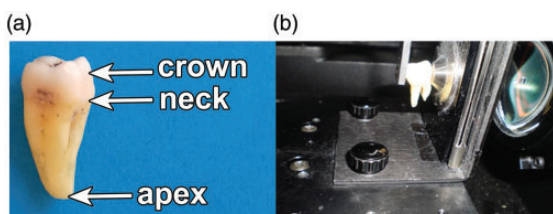


**Figure 2.** (a) Schematic representation of three sites on the external tooth surface from which Raman spectra were collected; (b) a tooth attached to the specimen holder with an aperture of  $d = 2.5$  mm which was used for defining the sampling surface.

function of donor's age indicates that a PCR model for age determination can be built.

The predictive capabilities of PCR models for age determination based on different spectra collection sites are summarized in Table IV. The highest coefficients of correlation and lowest error values were obtained in models based on apex spectra ( $R^2$  values of 0.84 and 0.71 for males and females, respectively). Models based on other

**Table II.** Designation of age groups for principal component analysis.

Group no.	Age (years)
1	10–19
2	20–29
3	30–39
4	40–49
5	50–59
6	60–69
7	70–79

combinations of genders and spectra collection sites had comparably lower  $R^2$  values, ranging from 0.17 to 0.59. Low  $R^2$  values (0.18–0.24) were also obtained for joint models that were built using spectra from both genders.

PCA loadings plots for PCI and PC2 are plotted with the corresponding representative spectra for each spectra collection site in Fig. 5. In models built from the apex spectra, only PCI loadings were different from zero (Fig. 5a), while for crown and neck, both PCI and PC2 loadings differed from zero (Figs. 5b and 5c). For all spectra collection sites, the contributions to first two principal components originated from both the organic and inorganic part of Raman spectra.

The regression plots for tooth donor's age and scatter-plots for the first two principal components are shown in Fig. 6, for each combination of gender and spectra collection site. The red lines in regression plots represent the actual correlation between measured and predicted values, while the green lines represent an ideal correlation. The PCA models based on apex spectra showed a comparatively better separation of age groups than the models based on neck and crown spectra. Accordingly, the PCR age determination models based on apex spectra showed higher coefficients of determination and lower error values compared to the models based on neck and crown spectra. The PCA scatterplots for apex indicate that age groups were separated only along the PCI axis (Figs. 6a and 6b). In the PCA model for male apex (Fig. 6a), younger age groups (10–39 years) were especially well separated from older age groups (40–79 years). Comparatively more overlapping between the age groups was found in the PCA model for female apex (Fig. 6b). In contrast to the PCA models for the apex, spectra from neck and crown were distinguishable by both PCI and PC2 (Fig. 6c to 6f).

## Discussion

In this study, Raman spectra of mineralized tooth tissues were used to build a PCR age determination model for forensic applications. The predictive capabilities of the



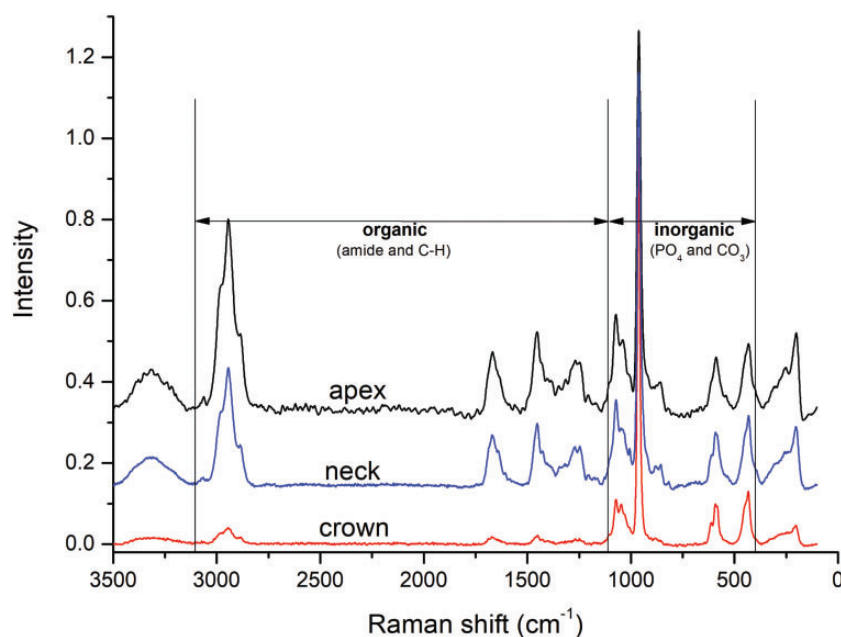


**Figure 3.** Representative Raman spectra collected from apex, crown, and neck. The spectra are normalized on the  $\text{PO}_4$  band at  $960\text{ cm}^{-1}$ .

**Table III.** Assignments of Raman vibrational bands.

Wavenumber ( $\text{cm}^{-1}$ )	Assignment
2940	C–H stretching mode
1665	Amide I (C=O)
1450	C–H bending mode
1242	Amide III (N–H)
1069	V3 asymmetric stretching mode of $\text{PO}_4$
1069	V1 symmetric stretching mode of type B $\text{CO}_3$
960	V1 symmetric stretching mode of $\text{PO}_4$
590	V4 asymmetric bending mode of $\text{PO}_4$
431	V2 symmetric bending mode of $\text{PO}_4$

obtained models varied according to the spectra collection site. Therefore, both research hypotheses were accepted.

The accuracy of regression models for age determination depends on the ratio of the variance attributable to aging-related changes and the uncontrolled variance due to various external factors and interindividual genetic differences. Relative magnitudes of these two sources of variance differed across the investigated sites at the tooth surface, thereby affecting the suitability of a particular site for age determination. High  $R^2$  values identified for apex indicate that a proper selection of spectra collection site can minimize uncontrolled variance. Comparatively poorer coefficients of determination were obtained for spectra collected at tooth neck and crown, indicating a higher magnitude of

uncontrolled variance at these sites. The differences in the suitability of different tooth sites for age determination can be explained by the distribution of different types of mineralized tissues across these sites. Three main mineralized tooth tissues include enamel, dentin, and cementum. These tissues differ by their fundamental physiological processes and the capability to respond to external stimuli, which affects their aging-related compositional changes.<sup>23</sup>

Enamel is the most highly mineralized tissue in the human body, with an inorganic content of 96 wt%. Enamel covers the tooth crown and is distinct from other mineralized tooth tissues because its formative cells are destroyed upon tooth eruption into the oral cavity.<sup>24</sup> As no cellular reparatory response is possible, the aging-related changes of enamel are completely under the influence of environmental factors and masticatory function. With aging, the enamel layer progressively becomes thinner due to chemo-mechanical degradation caused by erosive foods and chewing forces.<sup>25</sup> Additionally, the biofilm on the tooth surface harbors acidogenic bacteria which cause demineralization, i.e., loss of calcium and phosphate ions. The process of demineralization is counteracted by the remineralizing action of calcium and phosphate ions from the saliva.<sup>26</sup> These processes interchange cyclically, making the loss of ions fully reversible. However, if the net balance between remineralization and demineralization is negative for a prolonged period of time, enamel progressively loses its integrity and a carious lesion occurs. Between the sound and the carious state as the extremes, a whole range of intermediate demineralization stages is possible. The surface enamel layer in vivo usually presents various levels of

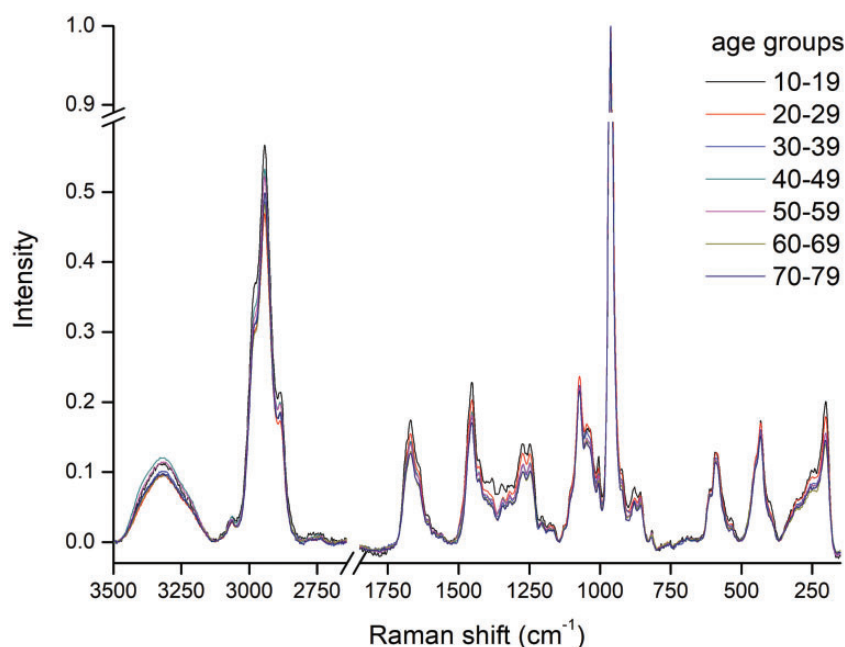


**Figure 4.** Average Raman spectra for seven age groups. The spectra were collected from the root apex of male donors. Note the breaks on the x- and y-axes.

**Table IV.** Characteristics and predictive capabilities of different PCR models: number of spectra on which the models were based, coefficient of determination ( $R^2$ ), root mean square error of calibration (RMSEC), and root mean square error of cross-validation (RMSECV).

Model	No. of spectra	$R^2$	RMSEC (years)	RMSECV (years)
Apex male	320	0.84	5.7	7.2
Apex female	390	0.71	7.3	8.1
Crown male	320	0.42	11.9	13.8
Crown female	390	0.43	10.6	11.5
Neck male	320	0.59	9.2	11.3
Neck female	390	0.17	13.9	14.0
Joint apex	710	0.24	14.3	14.6
Joint crown	710	0.22	14.5	14.7
Joint neck	710	0.18	14.6	14.9

mineralization which are heterogeneously distributed across the tooth surface.<sup>6</sup> This compositional heterogeneity is reflected in the Raman spectra of enamel<sup>9,11</sup> and introduces the uncontrolled variance that impairs the accuracy of the PCR model for age determination. Therefore, the low coefficients of determination obtained for the spectra collected from the crown can be attributed to the fact that enamel composition and structure were highly influenced by individual differences related to lifestyle, diet, and oral hygiene practice.<sup>27</sup>

Cementum is a mineralized tissue that covers the tooth root and increases in thickness towards the root apex. With approximately 65 wt% of inorganic and 25 wt% of organic content, cementum resembles the chemical composition of bone.<sup>28</sup> However, cementum is structurally different from bone as it is avascular and does not undergo continuous remodeling. Instead of remodeling, cementum is incrementally deposited by its formative cells (cementoblasts) throughout the lifetime.<sup>29</sup> Under physiological conditions, the recruitment of cementoblasts from progenitor cells and the deposition of cementum occurs at a steady pace.<sup>30</sup> The resulting compositional changes identified by Raman spectrometry appear to be consistent with aging, as indicated by high  $R^2$  values obtained for spectra collected from the apex. As a potential source of uncontrolled variance at that site, periodontal inflammatory processes should be considered. The periodontal inflammation (periodontitis) with the prevalence of up to 50% in the general population is one of the most common diseases in developed countries.<sup>31</sup> Periodontitis was also the most common reason for the extraction of teeth used in this study; 36 out of 71 teeth (51%) were extracted due to advanced periodontitis. The pathophysiology of periodontitis involves inflammation-mediated destruction of tooth-supporting tissues triggered by specific bacterial species. As the disease is often left untreated, chronic low-level inflammation can persist for years and affect the structure and composition of cementum. On the other hand, the periodontal treatment that involves mechanical scraping of the infected root surface also inflicts damage to cementum and affects the metabolic processes in cementoblasts. Consequently, either



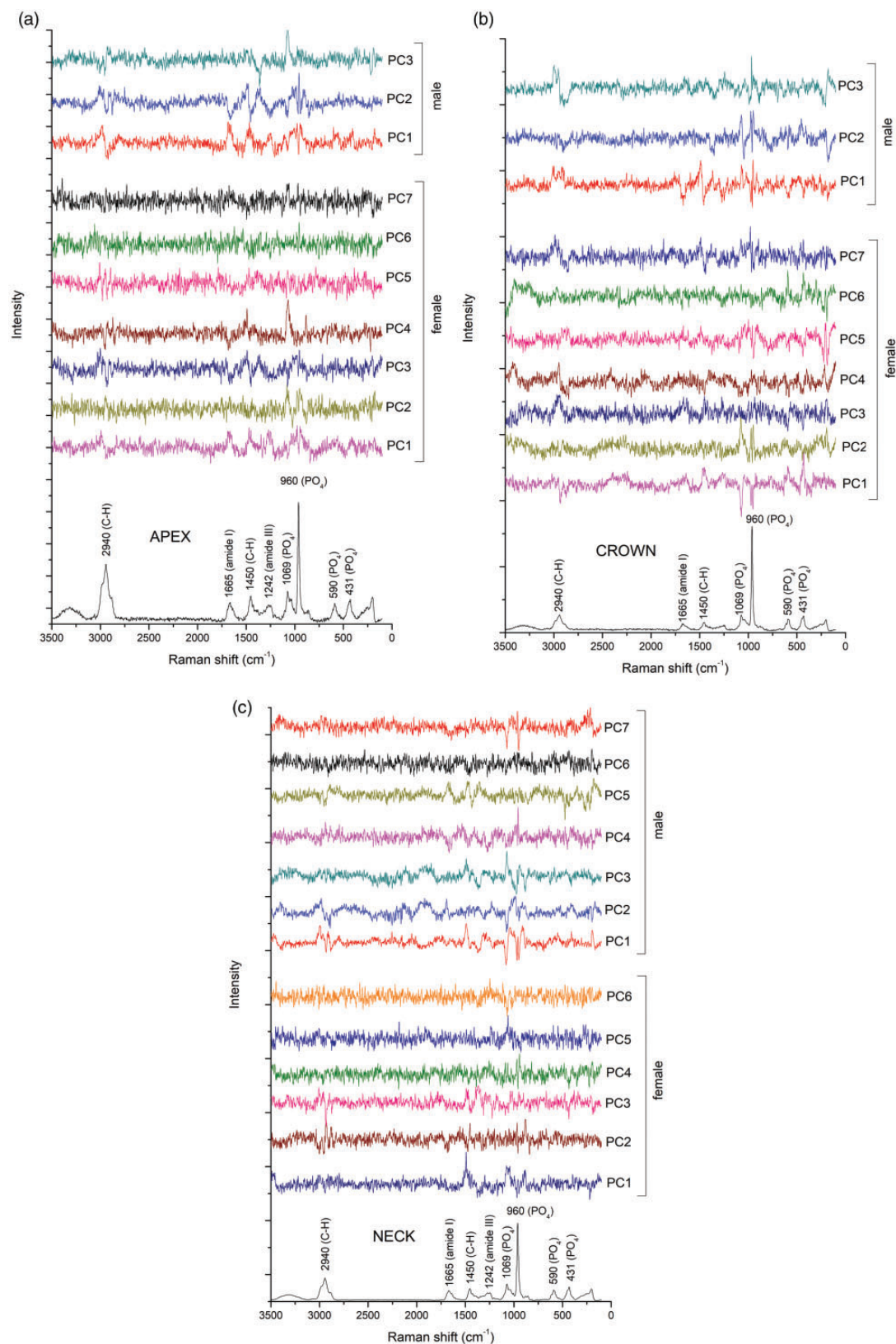


**Figure 5.** PCA loadings plots for the principal components used for age determination models, based on spectra collected from (a) apex, (b) crown, and (c) neck.

treated or untreated periodontal disease can affect the composition of cementum.<sup>32</sup> As periodontitis is initiated at the level of the tooth neck and gradually advances in the apical direction over the course of the disease, the

mineralized tissues at the tooth neck are more frequently and severely affected by the joint effect of periodontitis and periodontal treatment. Except in the most severe cases of periodontitis, the apical cementum remains unaffected.

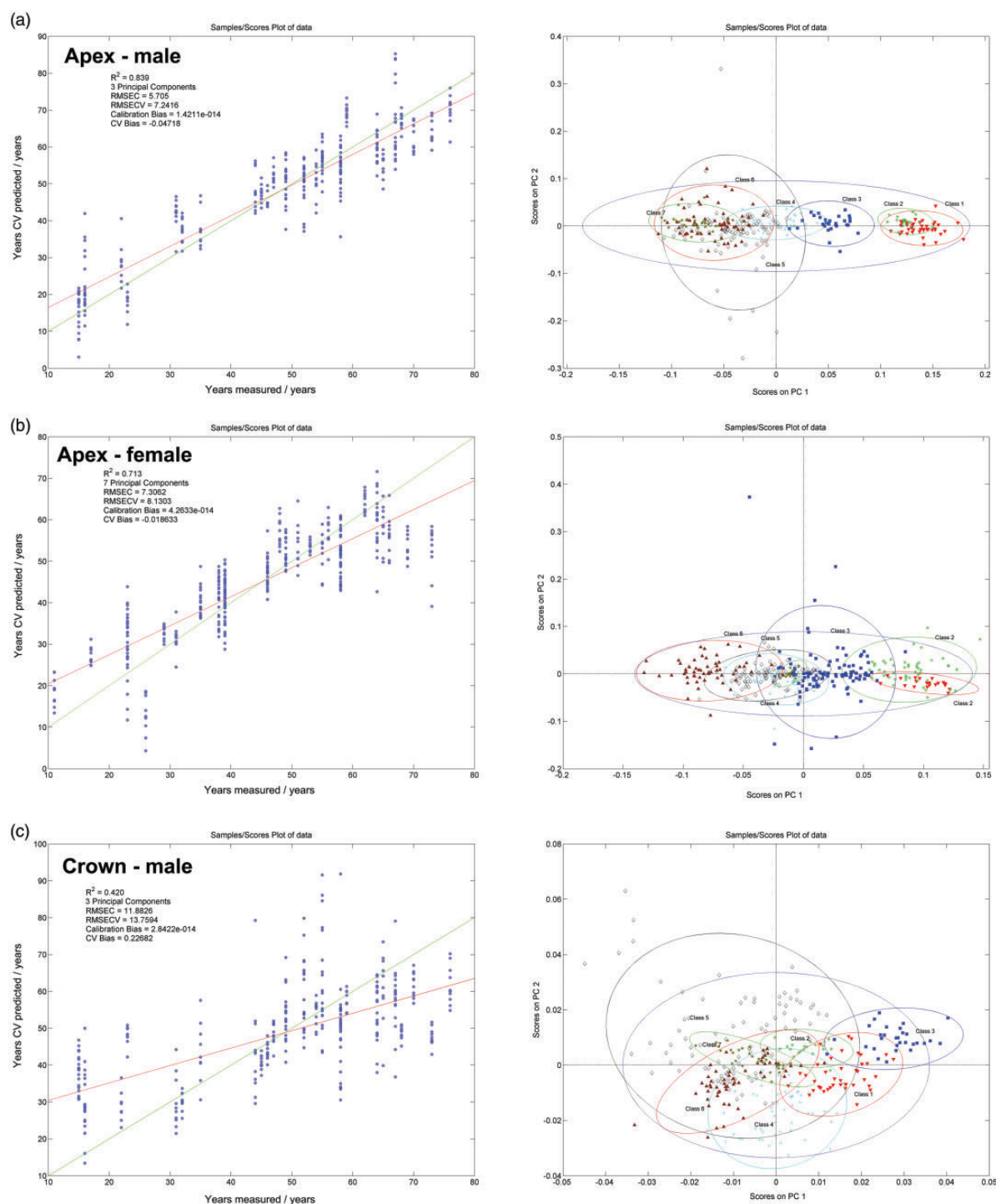


**Figure 6.** Regression plots and scatterplots for the first two principal components. The results are presented for models based on the following combinations of spectra collection site and gender: (a) apex male, (b) apex female, (c) crown male, (d) crown female, (e) neck male, and (f) neck female.

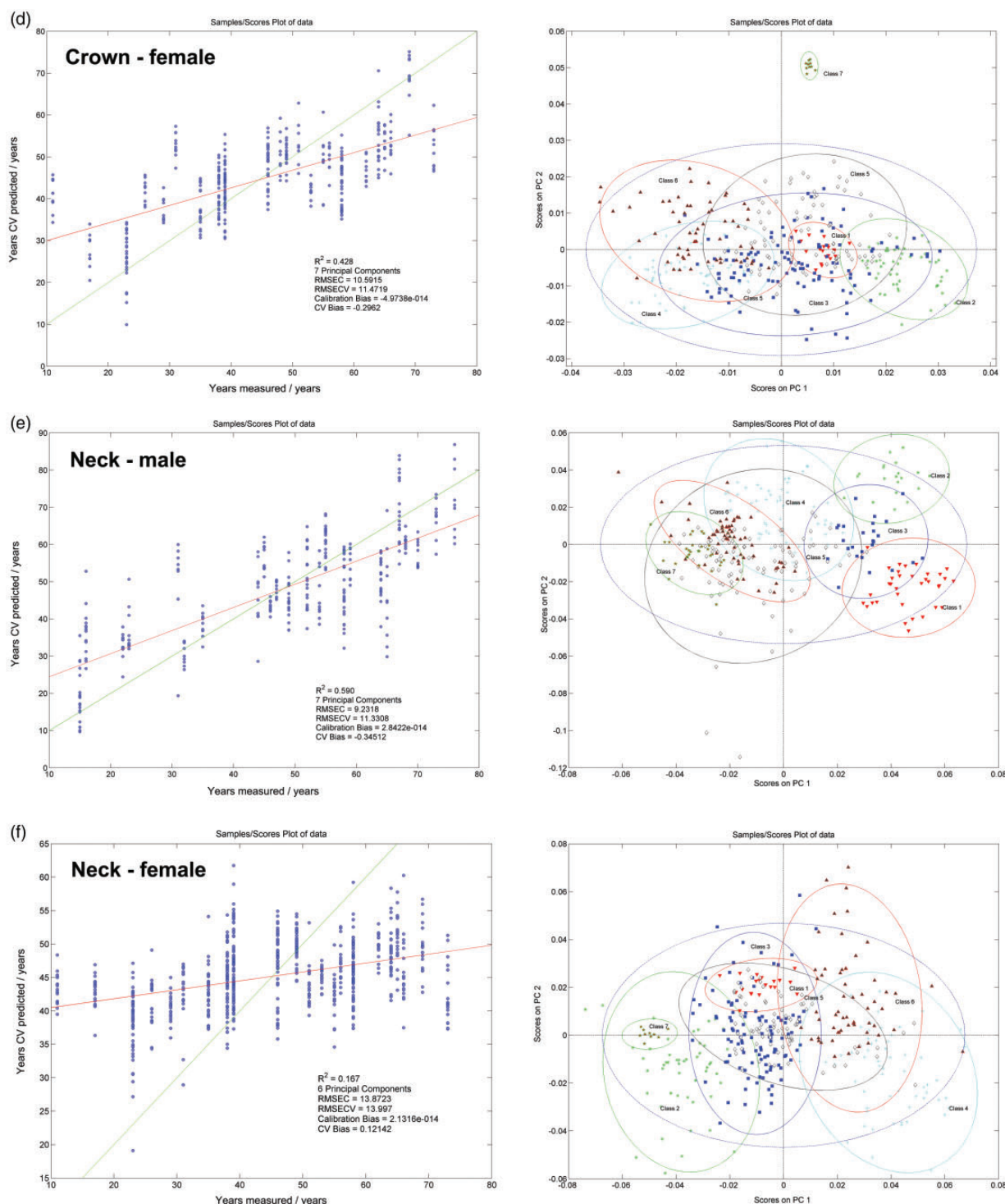


Figure 6. Continued.

The fact that apical cementum is mostly protected from external influences and is characterized by a steady rate of compositional changes renders root apex an appropriate spectra collection site for the age determination PCR model. Another factor that may affect the structure of

apical cementum is periodontal inflammation of endodontic origin, which is initiated and most pronounced around root apex.<sup>33</sup> Considering that 39% of the teeth used in this study were extracted due to failed endodontic treatment, this type of pathology was rather common in the analyzed

sample. However, it appears not to have significantly impaired the suitability of apical cementum as the tissue of choice for age determination.

Dentin is a mineralized tooth tissue with approximately 65 wt% of inorganic and 20 wt% of organic content. Dentin constitutes the bulk of the tooth and is covered by an enamel layer on the crown and a cementum layer on the root. The structure and composition of dentin are determined by the metabolic activity of its formative cells (odontoblasts) throughout the lifetime.<sup>34</sup> Despite having an acellular structure, dentin is permeated by tubules that contain cytoplasmic processes of odontoblasts located within the dental pulp. Over the lifetime, these cells continuously secrete minerals into the walls of dentinal tubules, leading to their narrowing, reduced permeability, and increased mineral content.<sup>35</sup> Under physiological conditions, dentin is fully covered by other mineralized tissues and protected from external influences. Therefore, compositional changes of dentin correlate well with donor's age, which has been exploited in two aforementioned studies employing Raman spectrometry for age determination.<sup>14,15</sup> In these studies, access to intact dentin was accomplished by tooth sectioning. Such access to dentin within the bulk of the tooth was not possible in the present study due to the nondestructive specimen preparation. However, areas of dentin were exposed on the tooth neck surface due to defects in overlying enamel and cementum. Dentin exposure on the tooth neck commonly occurs due to repeated damage of overlying enamel and cementum caused by masticatory loading, acid exposure, and aggressive tooth brushing.<sup>36</sup> Within the surface area exposed to the excitation laser (circular spot of  $d = 0.25$  mm), small areas of exposed dentin were sampled together with various fractions of enamel and cementum. Therefore, Raman spectra collected from the tooth neck contained contributions from all three types of mineralized tissues. The relative magnitudes of these contributions varied according to the extent of damage to overlying enamel and cementum, which was not quantified in the present study. The compositional heterogeneity of the mixture of mineralized tissues sampled at the tooth neck can explain the low predictive value of the PCR model based on spectra collected at that site. Also, the exposed dentin on the tooth neck exhibited faster mineral deposition and tubular occlusion as a part of the protective physiological response,<sup>37</sup> which introduced additional variance that was unrelated to aging.

Regarding apical cementum, which was identified as the most suitable tissue for age determination, it is interesting to note that PCR models based on apex spectra were more accurate for male than female donors. This might be related to the potential of female sex hormones to affect cementoblast metabolism, thereby introducing interindividual differences into the structure and composition of cementum. Although the effect of female sex hormones on cementoblast functions has not been well investigated,

cementoblasts are known to respond to estrogens.<sup>38</sup> Therefore, fluctuations in the levels of female sex hormones might be involved in the regulation of cementoblast function similarly to that in bone metabolism.<sup>39</sup> The individual variations in the production of female sex hormones and the corresponding cementoblast response can be speculated to have caused a lower accuracy of the age determination model for females.

The aging-related compositional changes in mineralized tissues that made the age determination model possible were identified in both the inorganic and the organic part of Raman spectra. These changes can be attributed to different processes occurring in tooth tissues with aging, including qualitative changes of calcium hydroxyapatite<sup>40</sup> and collagen,<sup>41</sup> as well as quantitative changes in the relative amounts of inorganic and organic components.<sup>42</sup> However, more detailed investigations of these processes through the analysis of principal component loadings were out of the scope of this study, which was focused on the practical application of Raman spectra for forensic age determination.

In teeth affected by various pathological processes, care was taken to collect Raman spectra from apparently intact tooth surfaces. While this approach helped to avoid areas severely affected by caries or covered by calculus, minor irregularities on the surface of mineralized tissues selected for the analysis might have remained unnoticed by visual inspection. A more precise microscopic inspection would allow better control over the quality of the sampled part of mineralized tissues; however, the naked-eye inspection was deliberately adopted as a part of the simplified and nondestructive specimen preparation. An additional rationale for not applying a strict selection of sound mineralized tissues was the study design simulating a realistic forensic scenario in which only a limited amount of material is available for analysis.

A major limitation of the present study is that the age determination model was based on teeth obtained exclusively from Caucasians, thereby not accounting for interethnic variations. It is reasonable to expect that age determination models would become less accurate if these were generalized to account for multiple races.<sup>43</sup> An additional shortcoming of the presented age determination model is that its predictive capability drops considerably if the gender of the donor is unknown. Therefore, for optimal accuracy of the age determination model described in this study, the gender and race of the tooth donor should be determined using other forensic methods.<sup>44</sup>

This study showed that whole Raman spectra obtained from the tooth surface using macro-Raman measurements can be used for age estimation. The quality of age-related information varied among tooth sites, and apical cementum showed the highest predictive potential. Although the obtained  $R^2$  values were relatively modest even for apical cementum, it was possible to improve these values for



more than 0.05 by removing 10% of outliers from the modeling set. This observation indicates that the precise definition of spectra recording conditions coupled with precise criteria for removing outliers can improve model precision. Such a refinement of age determination models will be addressed in our future studies.

Because Raman spectra of hydroxyapatite may be affected by laser light polarization,<sup>45,46</sup> it should be mentioned that for spectra collection in our study, both incident and scattered light were unpolarized. Therefore, possible influences of polarization were consistent within all spectra, thereby introducing the same type of error to all of them. Because the algorithms applied in this study are based on detecting relative differences between spectra, that error can be neglected.

In comparison to the previously published approaches based on the extraction of preselected parameters of individual Raman bands,<sup>14,15</sup> working with the whole Raman spectra for model building and later forensic application considerably simplifies the procedure. Additionally, macro-Raman measurements simulate spectra collection using a handheld Raman spectrometer, bringing the method closer to an actual forensic application. The age determination models built using spectra of unsound teeth have higher practical relevance than those based exclusively on intact teeth. Also, the spectra collection on the tooth surface is beneficial for forensic analysis, which generally favors nondestructive specimen handling.

To simulate a forensic scenario in which teeth at different postextraction time periods need to be analyzed, Raman spectra were collected 0.1–5.5 years after extraction. During the time period between extraction and spectra collection, the teeth were stored dry at room temperature. Mineralized tooth tissues remained well preserved under such conditions, whereas more extensive decomposition can be expected at higher temperatures or in highly acidic environments.<sup>47,48</sup> At this point, it is not possible to determine whether the age determination model presented in this study would be applicable to teeth that were aged under extreme conditions. However, mineralized tooth tissues are known to be resistant to a range of environmental effects of moderate intensity,<sup>1</sup> indicating a potential of hereby presented age determination method for use in contemporary forensic dentistry.

## Conclusion

This study showed that the age determination model based on principal component regression can be built using Raman spectra collected from surfaces of unsound teeth without any previous preparation. The optimal age determination capability was attained by using Raman spectra collected from cementum at root apex, whereas spectra collected from mineralized tissues at the tooth neck and crown were less suitable. The age determination model

based on apex spectra showed an optimal performance only when tooth donor genders were analyzed separately.

## Authors' note

The data sets generated during and/or analyzed during the current study are available from the corresponding author on reasonable request.

## Declaration of Conflicting Interests


The author(s) declared no potential conflicts of interest with respect to the research, authorship, and/or publication of this article.


## Funding

The author(s) received no financial support for the research, authorship, and/or publication of this article.

## ORCID iDs

Matej Par  <https://orcid.org/0000-0002-2846-1840>

Marko Škrabić  <https://orcid.org/0000-0003-1173-2162>

Ozren Gamulin  <https://orcid.org/0000-0001-6046-9773>

## References

1. I.A. Pretty, D. Sweet. "A Look At Forensic Dentistry – Part I: The Role of Teeth in the Determination of Human Identity". *Br. Dent. J.* 2001. 190(7): 359–366.
2. B. Rai, J. Kaur. *Evidence-Based Forensic Dentistry*. New York, NY: Springer; 2012.
3. M.A. Bush, P.J. Bush, R.G. Miller. "Detection and Classification of Composite Resins in Incinerated Teeth for Forensic Purposes". *J. Forensic Sci.* 2006. 51(3): 636–642. DOI: 10.1111/j.1556-4029.2006.00121.X.
4. K.C. Doty, C.K. Muro, J. Bueno, et al. "What Can Raman Spectroscopy Do for Criminalistics?" *J. Raman Spectrosc.* 2016. 47(1): 39–50. DOI: 10.1002/jrs.4826.
5. N.E. Pretorius, A. Power, M. Tennant, et al. "The Use of Vibrational Spectroscopy in the Geographic Characterization of Human Teeth: A Systematic Review". *Appl. Spectrosc. Rev.* 2020. 55(2): 105–127.
6. A. Akkus, A. Akkus, R. Roperto, et al. "Evaluation of Mineral Content in Healthy Permanent Human Enamel by Raman Spectroscopy". *J. Clin. Exp. Dent.* 2016. 8(5): E549–E549. DOI: 10.4317/jced.53057.
7. S.J. Fraser, A.K. Natarajan, A.S.S. Clark, et al. "A Raman Spectroscopic Study of Teeth Affected with Molar-Incisor Hypomineralisation". *J. Raman Spectrosc.* 2015. 46(2): 202–210. DOI: 10.1002/jrs.4635.
8. K. Bērziņš, J.J. Sutton, C. Loch, et al. "Application of Low-Wavenumber Raman Spectroscopy to the Analysis of Human Teeth". *J. Raman Spectrosc.* 2019. 50(10): 1375–1387.
9. T. Buchwald, Z. Okulus, M. Szybowicz. "Raman Spectroscopy as a Tool of Early Dental Caries Detection – New Insights". *J. Raman Spectrosc.* 2017. 48(8): 1094–1102. DOI: 10.1002/jrs.5175.
10. W. Hill, V. Petrou. "Detection of Caries and Composite Resin Restorations by Near-Infrared Raman Spectroscopy". *Appl. Spectrosc.* 1997. 51(9): 1265–1268. DOI: 10.1366/0003702971942088.
11. A.C.-T. Ko, L.-P. Choo-Smith, M. Hewko, et al. "Ex Vivo Detection and Characterization of Early Dental Caries by Optical Coherence Tomography and Raman Spectroscopy". *J. Biomed. Opt.* 2005. 10(3): 031118DOI: 10.1117/1.1915488.
12. C.P. Torres, J. Miranda Gomes-Silva, M.A.H. Menezes-Oliveira, et al. "FT-Raman Spectroscopy,  $\mu$ -EDXRF Spectrometry, and Microhardness

- Analysis of the Dentin of Primary and Permanent Teeth". *Microsc. Res. Tech.* 2018. 81(5): 509–514. DOI: 10.1002/jemt.23005.
13. E. Wentrup-Byrne, C.A. Armstrong, R.S. Armstrong, et al. "Fourier Transform Raman Microscopic Mapping of the Molecular Components in a Human Tooth". *J. Raman Spectrosc.* 1997. 28(2–3): 151–158. DOI: 10.1002/(SICI)1097-4555(199702)28:2/3<151::AID-JRS71>3.0.CO;2-5.
  14. P. Tramini, B. Bonnet, R. Sabatier, et al. "A Method of Age Estimation Using Raman Microspectrometry Imaging of the Human Dentin". *Forensic Sci. Int.* 2001. 118(1): 1–9. DOI: 10.1016/S0379-0738(00)00352-2.
  15. K. Kumari, R.S. Rao, S.C. Sarode, et al. "Raman Microspectrometry: An Alternative Method of Age Estimation from Dentin and Cementum". *J. Clin. Diagn. Res.* 2017. 11(10): 11–16. DOI: 10.7860/JCDR/2017/31161.10705.
  16. H. Martens, M. Hoy, B.M. Wise, et al. "Pre-Whitening of Data by Covariance-Weighted Pre-Processing: Pre-Whitening of Spectra". *J. Chemom.* 2003. 17(3): 153–165. DOI: 10.1002/Cem.780.
  17. U.K. Acharya, K.B. Walsh, P.P. Subedi. "Robustness of Partial Least-Squares Models to Change in Sample Temperature: I. A Comparison of Methods for Sucrose in Aqueous Solution". *J. Infrared Spectrosc.* 2014. 22(4): 279–286. DOI: 10.1255/Jnirs.1113.
  18. C.S. Silva, M.F. Pimentel, J.M. Amigo, et al. "Chemometric Approaches for Document Dating: Handling Paper Variability". *Anal. Chim. Acta.* 2018. 1031: 28–37. DOI: 10.1016/J.Aca.2018.06.031.
  19. M.G. Nespeca, G.B. Piassalonga, J.E. De Oliveira. "Infrared Spectroscopy and Multivariate Methods as a Tool for Identification and Quantification of Fuels and Lubricant Oils in Soil". *Environ. Monit. Assess.* 2018. 190(2): 72. DOI: 10.1007/s10661-017-6454-9.
  20. R. Ramakrishnaiah, G. Ur Rehman, S. Basavarajappa, et al. "Applications of Raman Spectroscopy in Dentistry: Analysis of Tooth Structure". *Appl. Spectrosc. Rev.* 2015. 50(4): 332–350. DOI: 10.1080/05704928.2014.986734.
  21. W.H. Arnold, P. Gaengler. "Quantitative Analysis of the Calcium and Phosphorus Content of Developing and Permanent Human Teeth". *Ann. Anat.* 2007. 189(2): 183–190. DOI: 10.1016/J.Aanat.2006.09.008.
  22. X.-F. Dai, A.R.T. Cate, H. Limeback. "The Extent and Distribution of Intratubular Collagen Fibrils in Human Dentine". *Arch. Oral Biol.* 1991. 36(10): 775–778. DOI: 10.1016/0003-9969(91)90045-V.
  23. D.R. Morse, J.V. Esposito, R.S. Schoor, et al. "A Review of Aging of Dental Components and a Retrospective Radiographic Study of Aging of the Dental Pulp and Dentin in Normal Teeth". *Quintessence Int.* 1991. 22(9): 711–720.
  24. C.E. Smith. "Cellular and Chemical Events During Enamel Maturation". *Crit. Rev. Oral Biol. Med.* 1998. 9(2): 128–161. DOI: 10.1177/10454411980090020101.
  25. M.C.D.N.J.M. Huysmans, H.P. Chew, R.P. Ellwood. "Clinical Studies of Dental Erosion and Erosive Wear". *Caries Res.* 2011. 45(S1): 60–68. DOI: 10.1159/000325947.
  26. N.J. Cochrane, F. Cai, N.L. Huq, et al. "New Approaches to Enhanced Remineralization of Tooth Enamel". *J. Dent. Res.* 2010. 89(11): 1187–1197. DOI: 10.1177/0022034510376046.
  27. A.A. Kunin, A.Y. Evdokimova, N.S. Moiseeva. "Age-Related Differences of Tooth Enamel Morphochemistry in Health and Dental Caries". *EPMA J.* 2015. 6(3): 1–11. DOI: 10.1186/S13167-014-0025-8.
  28. D.D. Bosshardt, K.A. Selvig. "Dental Cementum: The Dynamic Tissue Covering of the Root". *Periodontol* 2000. 1997. 13(1): 41–75. DOI: 10.1111/J.1600-0757.1997.Tb00095.X.
  29. P. Gupta. "Human Age Estimation from Tooth Cementum and Dentin". *J. Clin. Diagn. Res.* 2014. 8(4): 7–10. DOI: 10.7860/JCDR/2014/7275.4221.
  30. P.F. Gonçalves, E.A. Sallum, A.W. Sallum, et al. "Dental Cementum Reviewed: Development, Structure, Composition, Regeneration and Potential Functions". *Braz. J. Oral Sci.* 2005. 4(12): 651–8.
  31. A. Hugoson, O. Norderyd. "Has the Prevalence of Periodontitis Changed During the Last 30 Years?" *J. Clin. Periodontol.* 2008. 35: 338–345. DOI: 10.1111/J.1600-051X.2008.01279.X.
  32. W.J. Grzesik, A.S. Narayanan. "Cementum and Periodontal Wound Healing and Regeneration". *Crit. Rev. Oral Biol. Med.* 2002. 13(6): 474–484. DOI: 10.1177/1544111130201300605.
  33. M. Laux, P.V. Abbott, G. Pajarola, et al. "Apical Inflammatory Root Resorption: A Correlative Radiographic and Histological Assessment". *Int. Endod. J.* 2000. 33(6): 483–493. DOI: 10.1046/J.1365-2591.2000.00338.X.
  34. V.E. Arana-Chavez, L.F. Massa. "Odontoblasts: The Cells Forming and Maintaining Dentine". *Int. J. Biochem. Cell Biol.* 2004. 36(8): 1367–1373. DOI: 10.1016/J.Biocyel.2004.01.006.
  35. M. Goldberg. "Dentin: Structure, Composition, and Mineralization". *Front. Biosci.* 2011. E3(2): 711–735. DOI: 10.2741/E281.
  36. D.W. Bartlett, P. Shah. "A Critical Review of Non-Carious Cervical (Wear) Lesions and the Role of Abfraction, Erosion, and Abrasion". *J. Dent. Res.* 2006. 85(4): 306–312. DOI: 10.1177/154405910608500405.
  37. B. Van Meerbeek, M. Braem, P. Lambrechts, et al. "Morphological Characterization of the Interface Between Resin and Sclerotic Dentine". *J. Dent.* 1994. 22(3): 141–146. DOI: 10.1016/0300-5712(94)90197-X.
  38. J. Nuñez, S. Sanz-Blasco, F. Vignoletti, et al. "17 $\beta$ -Estradiol Promotes Cementoblast Proliferation and Cementum Formation in Experimental Periodontitis". *J. Periodontol.* 2010. 81(7): 1064–1074. DOI: 10.1902/Jop.2010.090678.
  39. H.K. Väänänen, P.L. Härkönen. "Estrogen and Bone Metabolism". *Maturitas.* 1996. 23(Suppl): S65–S69.
  40. T.H. Leventouri, A. Antonakos, A. Kyriacou, et al. "Crystal Structure Studies of Human Dental Apatite as a Function of Age". *Int. J. Biomater.* 2009. 2009: 1–6. DOI: 10.1155/2009/698547.
  41. A. Nazari, D. Bajaj, D. Zhang, et al. "Aging and the Reduction in Fracture Toughness of Human Dentin". *J. Mech. Behav. Biomed. Mater.* 2009. 2(5): 550–559. DOI: 10.1016/J.jmbbm.2009.01.008.
  42. P.J. Carrigan, D.R. Morse, M.L. Furst, et al. "A Scanning Electron Microscopic Evaluation of Human Dentinal Tubules According to Age and Location". *J. Endod.* 1984. 10(8): 359–363. DOI: 10.1016/S0099-2399(84)80155-7.
  43. D.R. Senn, P.G. Stimson. *Forensic Dentistry*. Boca Raton, FL: CRC Press, 2010.
  44. P.G. Stimson, C.A. Mertz. *Forensic Dentistry*. Boca Raton, FL: CRC Press, 1997.
  45. A.C.-T. Ko, L.-P. Choo-Smith, M. Hewko, et al. "Detection of Early Dental Caries Using Polarized Raman Spectroscopy". *Opt. Express.* 2006. 14(1): 203. DOI: 10.1364/OPEX.14.000203.
  46. H. Tsuda, J. Arends. "Orientational Micro-Raman Spectroscopy on Hydroxyapatite Single Crystals and Human Enamel Crystallites". *J. Dent. Res.* 1994. 73(11): 1703–1710. DOI: 10.1177/00220345940730110501.
  47. J.L. Ferreira, Á.E. De Ferreira, A.I. Ortega. "Methods for the Analysis of Hard Dental Tissues Exposed to High Temperatures". *Forensic Sci. Int.* 2008. 178(2–3): 119–124. DOI: 10.1016/J.forsciint.2007.12.009.
  48. I. Manolescu, A. Ion, B.G. Ioan. "Post-Mortem Changes in Teeth-Forensic Issues". *Int. J. Med. Dent.* 2015. 5(4): 5.